https://doi.org/10.2352/issn.2169-2629.2020.28.51

Estimation of Layered Ink Layout to reproduce desired Translucency of skin in Inkjet 3D Printer using deep neural network trained with synthetic simulated data

Kensuke Fukumoto[1)], Kazuki Nagasawa[1)], Wataru Arai [2)], Kunio Hakkaku [2)], Satoshi Kaneko [2)], Keita Hirai [1)], Norimichi Tsumura[1)]

1) Graduate School of Science and Engineering, Chiba University, CHIBA, JAPAN
2) MIMAKI ENGINEERING CO., LTD., NAGANO, JAPAN

Abstract

In this paper, we propose a method to estimate ink layer layout used as an input for 3D printer. This method makes it possible to reproduce a 3D printed patch that gives a desired translucency, which is represented as Line Spread Function (LSF) in this study. Deep neural networks of encoder decoder model is used for the estimation. In a previous research, it is reported that machine learning method is effective to formulate the complex relationship between the optical property such as LSF and the ink layer layout in 3D printer. However, it may be difficult to collect data large enough to train a neural network sufficiently. Especially, although 3D printer is getting more and more widespread, the printing process is still time consuming. Therefore, in this research, we prepare the training data, which is the correspondence between LSF and ink layer layout in 3D printer, by simulating it on a computer. MCML was used to perform the simulation. MCML is a method to simulate subsurface scattering of light for multi-layered media. Deep neural network was trained with the simulated data, and evaluated using a CG skin object. The result shows that our proposed method can estimate an appropriate ink layer layout which reproduce the appearance close to the target color and translucency.

1. Introduction

Optical properties are very important to describe objects. Optical properties are defined as the response of an object to electromagnetic waves, such as absorption, reflection, and transmission. A point spread function (PSF) and a line spread function (LSF) are examples of optical properties. When a translucent object is irradiated with light using a point or line light source, it is observed that the light spreads around the irradiation point. This is because light enters the interior of the object and repeats internal scattering, and light is emitted at a position different from the point of incidence. The plot of this light spread is the point spread function. These functions make it possible to describe the transparency of the object.

In recent years, three dimensional (3D) printers have become widely used and a lot of researches has been done related to that. A method called error diffusion halftoning for achieving tonal representation in conventional 2D printing has been extended for 3D printers[1], which enables detailed tonal representation. Furthermore, in recent research [2], a method using RGBA signals instead of BSSRDF, which is more expensive to measure and process, has been proposed as a method for full-color modeling with spatially varying translucency. Here, A is a signal for translucency. Accuracy has been further improved by research [3] that optimizes this A signal to link it to both optical material properties and human perceptual uniformity, independent of hardware and software. All the researches contributes to make it possible to reproduce desired material appearance in 3D printing. The point or line spread function mentioned in prebious paragraph is also a subject of interest related to 3D printing. It represents the spread of light caused by the internal scattering of a translucent object. This phenomenon can be reproduced by using clear ink and the density adjustment of the layer structure of an inkjet 3D printer.

In a 2D printer, the only input is the density of the ink used at each point, which is expressed as a digital image. However, in a 3D printer, the layer structure increases the degree of freedom in the depth direction, which complicates the problem. If the ink density of each layer and the resulting transparency can be controlled when performing 3D printing, any transparency can be reproduced as desired. In fact, Yoshii et al. proposed a method to estimate the density (ink layout) of the layer structure in a 3D printer to reproduce the desired translucency of human skin [4]. In their method, deep neural network is used where a line spread function is an input, and the ink layout of the 3D printer is output. It was shown that a method using machine learning was effective in estimating the relationship between the complex internal scattering of light caused by the layer structure and the density layout in 3D printing. However, in general, the difficulty which happens when adopting a method like machine learning is that large data is required to train the model sufficiently. Although the 3D printer is widely used these days, the printing process is much more time consuming compared to conventional 2D printers, which is why it is hard to modify the dataset and increase the number of data. Therefore, in this research, we propose a method to prepare the data in a flexible and efficient approach. Training data is synthesized on a computer using a simulation method, and a neural network is trained with it.

2. Related Works

In recent years, 3D printers have become widespread. In particular, inkjet 3D printers are paid attention to, which can depict a wide color gamut and can form translucent objects taking advantage of clear ink. However, it depends on the skill and experience of a designer how accurately the desired appearance is reproduced. The degree of freedom of modeling due to the 3D layer structure makes it difficult to determine the exact ink layer layout. Then, Yoshii et al. proposed a method to determine a layout that reproduces an arbitrary translucency using machine learning [4]. Figure 1 shows the outline of Yoshii's research. In their method, the input to the neural network is a line spread function (LSF) [5], which is an index indicating translucency. First, a skin patch is printed with a 3D printer, from which LSF is measured.

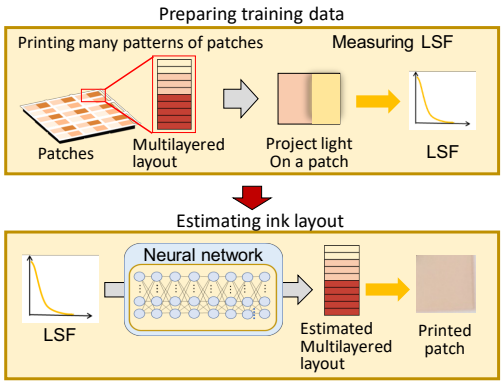

Figure 1. *The outline of related work[1]*

The obtained LSF is used for training a neural network. The ink concentrations and layer layout, which will be the input to the printer, need to be determined first. The layout was determined by referring to the actual structure of human skin. For the sake of simplicity, the complex skin structured is divided into the two main components, epidermis and dermis. There are no blood vessels in the epidermis layer and blood vessels in the dermis layer. Following this, 14 patterns of concentration of each ink were chosen in total; 10 patterns for skin color representing the epidermis, three patterns for red representing the dermis, and one pattern for clear ink controlling the translucency. Note that, in this research, the epidermis is assumed to have a typical Asian color. One each pattern was selected from them, and the order of the ink layer layout was fixed as clear, skin color, and red in order from the top. The total number of layers was set to 10 to prevent the patch from getting quite dark. Some ink layer layouts consist of only one or two patterns of ink concentration. These conditions resulted in a total of 1875 patches. From these skin patches, LSF was obtained and used as an index of translucency. The neural network was trained with the obtained data. This neural network outputs an ink layer layout, which reproduces similar LSF to the one given as the input. It is shown their method works very well; however, the procedure of preparing many skin patches with a 3D printer and calculating the LSF from it is still time-consuming. Therefore, in this research, we propose a method to prepare the data in a flexible and efficient approach. Training data is synthesized on a computer using a simulation method, and a neural network is trained with it.

3. *Estimating Parameters of Subsurface scattering using dipole model*

In this study, we simulate the layered structure of ink produced by a 3D printer on a computer and obtain the LSF. The simulation is performed using a method called MCML[6], which is used to simulate light scattering in multilayer structures. In order to perform MCML two parameters, the absorption and scattering coefficients are required. In this section, we describe a method for estimating these parameters from actual ink by fitting them using a dipole model, which is an optical model of subsurface scattering.

3.1 Dipole model

When light enters the interior of an object, it is emitted from the surface of the object after repeating collisions with absorbing and scattering materials in it. Therefore, the point at which light enters and exits is different. The BSSRDF (Bidirectional Scattered Surface Reflectance Distribution Function) is a function to formulate this phenomenon. The dipole model [7] is one of the models of BSSRDF. In the dipole model, BSSRDF is expressed as the following equation.

$$S(x_i, \vec{w}_i, x_o, \vec{w}_o) = \frac{1}{\pi} F_t(\eta, \vec{w}_i)\, R_d(x_i, x_o)\, F_t(\eta, \vec{w}_o) \quad (1)$$

In equation (1), $x_i, \vec{w_i}$ is the position and direction of the incident light and $x_o, \vec{w_o}$ is the position and direction of the outgoing light. η is the relative refractive index. F_t is the Fresnel transmittance. R_d is the scattering term, which indicates the extent to which the light expands from the point of incidence. The equation of the dipole model has the parameters, the scattering and absorption coefficients σ_s and σ_a, the anisotropy parameter g, and the relative refractive index η. These parameters can be estimated by observing the spread of light inside an object and fitting it to a dipole model. A laser projector (Smart Beam Laser, United Object) was used as a light source. This projector consists of RGB lasers with the spectrum shown in Figure 2. Figure 3 shows the setup for imaging the ink sample. The photograph was taken under the darkroom. A SONY α5100 camera was used and a polarizer was attached in front of the lens to remove the surface reflection on the sample. The resolution of the image is 6000×4000.

3.2 Measuring Subsurface scattering of Ink samples

An ink sample is irradiated with light and the spread of the light is observed. Figure 4 shows a photograph of samples of ink printed with a 3D inkjet printer. In Figure 4, the inks are cyan (C), magenta (M), yellow (Y), black (K), clear (Clear), and white (W) in order from the right.

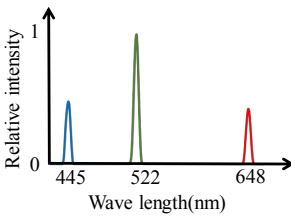

Figure. 2 *Spectrum of Smart Beam Laser Projectors*

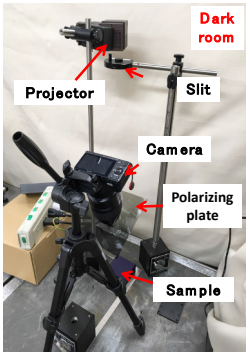

Figure. 3 *The setup for imaging the ink sample*

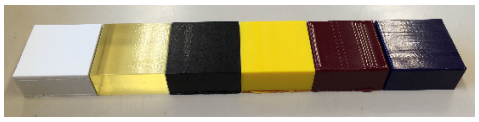

Figure. 4 *samples of ink printed with a 3D inkjet printer.*

A pseudo point light source was reproduced by projecting an image whose center is white through a slit. Each sample was taken in seven shots with exposure times of 1/1000, 1/250, 1/60, 1/15, 1/4, 1, and 4 to make an HDR image. The purpose of the HDR processing is to obtain a small luminance value produced by the scattered light in the sample. Figure 5 shows the captured images of the yellow sample as an example. Note that for simplicity, the point spread function of the camera lens and reflections at the air-matter interface are ignored.

3.3 Fitting the obtained sample data to dipole model

We estimate the parameters by fitting the data taken in the previous section to the dipole model. There are four parameters to be estimated: absorption and scattering coefficients, anisotropy parameters, and relative refractive index. In this paper, we assume that the ink to be estimated is isotropic, and the value of the anisotropy parameter g is set to 0. Since the relative refractive index is known to take a value of 1.3 for most materials, we use that value. Therefore, there are only two targets for the estimation: the absorption and scattering coefficients.

In the image obtained by taking a sample, where the incident position of the laser light source is x_i and the distance from it is r_i and the corresponding pixel value is p_i, p_i can be expressed by the following equation using the radiation flux Φ of the light source and the unknown constant K.

$$p_i = K\Phi R_d(r_i) \tag{2}$$

The value of $R_d(r_i)$ is required for fitting to the dipole model. To obtain it from Equation (2), we first need the values of K and Φ. The sum of the pixel values of the image taken by projecting a laser beam onto spectralon is calculated to be $K\Phi$ divided by A. Here, A is the actual area in pixels in the taken image. It was calculated by taking a picture of a sample that has a ruler on it. By obtaining these values, we can calculate the value of $R_d(r_i)$, which is the scattering term of the dipole model. The procedures described above are used to obtain the scattering terms of the dipole model and fit them to the function. For the fitting, we used the curve_fit function implemented in scipy, a python module. As fitting conditions, the range of absorption and scattering coefficients was set to be greater than or equal to 0, and the default values were used for the initial value of the optimization. Examples of fitting are shown in Figure 6. Figure 6(a) shows the results of fitting to the image of the R component of the yellow ink sample. The horizontal axis of the graph is the distance from the point where the laser beam is injected (origin), and the vertical axis is the scattering term. The red circles in the figure are the scattering terms obtained from the captured images, and the blue curves are the fitted curves. It can be seen that the estimation of the parameters is mostly correct. However, the estimation of the magenta ink sample shown in Figure 6(b) for the B component appears to be inaccurate. In the dipole model, the scattering coefficient is assumed to be sufficiently high compared to the absorption coefficient, otherwise, the accuracy will be low. Therefore, we conducted to correct the parameters based on the values obtained from the fitting of the dipole model.

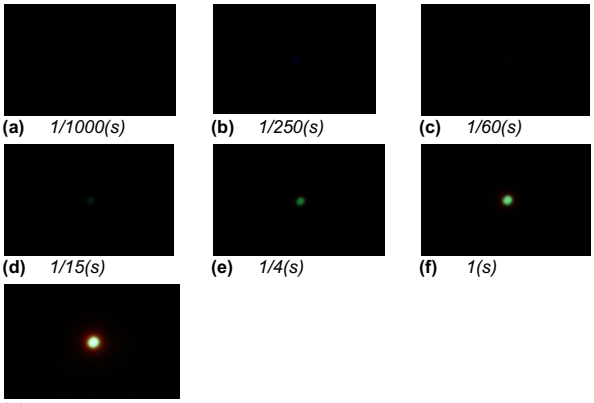

(a) *1/1000(s)* **(b)** *1/250(s)* **(c)** *1/60(s)*
(d) *1/15(s)* **(e)** *1/4(s)* **(f)** *1(s)*
(g) *Exposure time: 4(s)*

Figure. 5 *The result of capturing the light scattering of the yellow sample with different exposure time.*

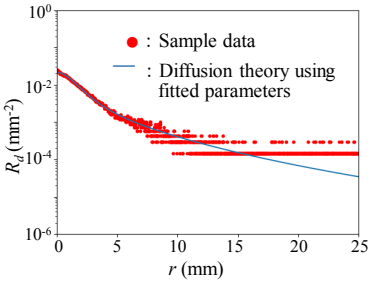

(a) *R component of yellow sample*

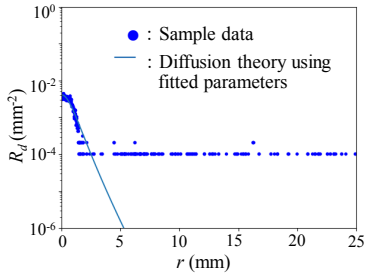

(b) *B component of magenta sample*

Figure. 6 *The examples of fitting*

3.4 Parameters correction

In the previous section, we estimated the absorption and scattering coefficients. However, in parameter estimation using dipole models, the accuracy is poor when the values of the absorption coefficients are relatively larger than the scattering coefficient. Therefore, in this section, the spectral reflectance factor of the ink samples is measured, and the parameters are corrected based on the values. For each ink sample shown in Figure 4, the spectral brightness is measured using a spectral radiometer (TOPCON's SR3). At the same time, the spectral radiance of a spectralon is measured and the spectral reflectance factor is calculated by dividing the measurement for each sample by the value. The measurements were conducted under a dark room, and a white bulb was used as the light source. Surface reflection was

removed by attaching polarizers on the light source and lens, respectively. Since clear ink showed an obvious absorption phenomenon, a standard white plate was placed on the back of the sample to reflect the light after transmission, and the absorption rate of the sample was obtained. Here, there are innumerable combinations of absorption and scattering coefficients that give a certain reflectance in MCML. Therefore, we fix the scattering coefficients of the RGB components of each ink sample estimated previously assuming that they are correct. MCML was performed repeatedly with the fixed scattering coefficients and different absorption coefficients and the values were adopted when the obtained reflectance by MCML and the measured reflectance by spectral radiometer gets close enough. Note that this MCML performed here is for parameter correction, not for obtaining the LSF of the skin patch. In order to match the reflectance, it is necessary to select a wavelength that is representative of the RGB value, and the wavelength of the smart beam laser is adopted. For the black ink samples, the scattering coefficient was set to a sufficiently low value (0.01) and the absorption coefficients were calculated in the same way as for the other inks. Assuming that some scattering occurs for clear ink, we set the value of the scattering coefficient of SKIN1 in the literature [7] to obtain the absorption coefficient. In order to perform the simulation using MCML in the same situation as the spectral reflectance measurements, we added a layer having a sufficiently high scattering coefficient and no absorption underneath the clear ink layer.

4. A simulation *using MCML* to *Reproduce ink patches and Obtain Line spread function*

In the previous section, the values of absorption and scattering coefficients for each ink sample were obtained, and the conditions for performing MCML were satisfied. In this chapter, the settings for the simulation are explained and the obtained LSF is described.

4.1 The conditions in the simulation

In MCML, the thickness and volume concentration of each layer can be set. In this case, we match the settings to the skin patch actually printed in the previous study described in Chapter 2. A total of 14 ink concentration patterns (1 clear ink, 3 skin inks, and 10 red inks) were prepared for the skin patch, and 10 layers of these patterns were combined to create the skin patch. A figure illustrating this is shown in Figure 7. Printers can only control whether the ink is applied to a dot or not, and cannot change the concentration of the ink itself, and to control the concentration, the proportion of ink in the area is changed by halftoning. In MCML, it is difficult to reproduce this area representation of concentration. Therefore, we consider it as a mixture of inks and express the concentration in terms of volume. In the simulation, the thickness of each ink was matched to 30 μm, which is the thickness of a single dot of ink output by a real 3D printer. The lowermost layer was set as a base layer with a sufficiently high scattering coefficient.

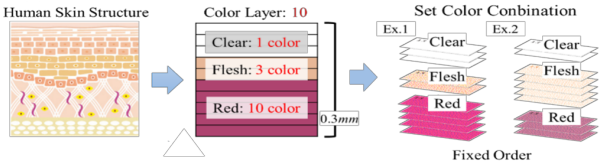

Figure. 7 *Conditions to determine the structure of ink layer layout for human skin color patches* [1]

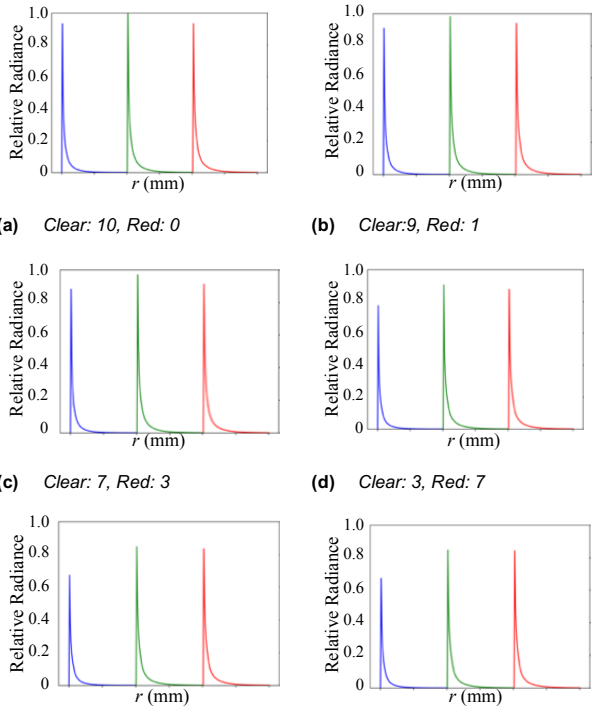

(a) *Clear: 10, Red: 0* **(b)** *Clear:9, Red: 1*

(c) *Clear: 7, Red: 3* **(d)** *Clear: 3, Red: 7*

(e) *Clear: 1, Red: 9* **(f)** *Clear: 0, Red: 10*

Figure. 8 *examples of LSF obtained by the MCML simulation*

4.2 The result of the simulation

Figure 8 shows an example of the results obtained by the MCML simulation. In Figure 8, the LSF for each RGB component is shown in each image. The horizontal axis is the distance from the incident point, and the vertical axis is the relative intensity of the reflection, which was normalized to make the range from 0 to 1. It was seen in the result that the relative intensity at the actual incident point was extremely large compared to the others. That is why in calculating the LSF, we assumed a point 0.2 mm away from the incident point as the incident point so that the spread of the light can be easily observed. For the red ink, one of the ten patterns of ink concentration was chosen. From Figure 8, it can be seen that as the number of red ink layers increases from (a) to (f), the overall peak of the LSF decreases. In particular, the decline of the B component is greater than that of the other components. This is thought to be due to the increased absorption of the B component by increasing the number of layers of red ink.

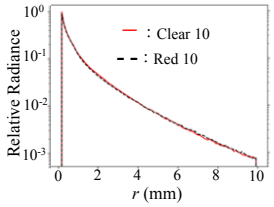

(a) *R component*

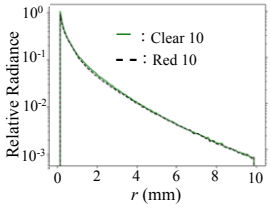

(b) *G component*

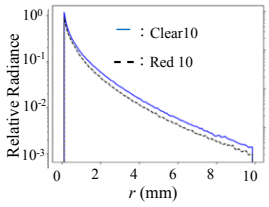

(c) *B component*

Figure. 9 *The LSF shown in (a) and (f) in Figure 8 on a log scale.*

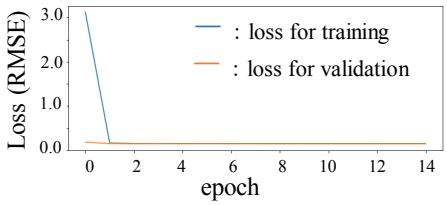

(a) *Learning curve of decoder*

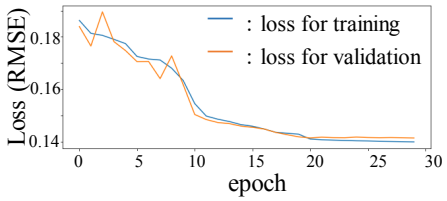

(b) *Learning curve of encoder*

Figure. 11 *Learning curves of neural networks*

Figure 9 is the LSF shown in (a) and (f) in Figure 8 on a log scale. In Fig. 9, the attenuation of the R and G components is almost unchanged due to the difference in layout, but in the B component, the attenuation is relatively steeper for the 10 layers of red ink.

5. Deep Neural Network Model

In the previous chapter, we used MCML to synthesize the skin patches on the computer. In this chapter, these data are used as training data. Using the trained neural networks, given an LSF, we estimate the ink layer layout of a 3D printer that reproduces it.

5.1 The structure of Deep neural network model

The purpose of this study is to estimate a layout that reproduces a given LSF. However, it is difficult to determine how accurate one estimated layout is compared to another. For such problems, an encoder and decoder type of neural network shown in Fig. 10 is effective [8, 9]. This model was used in a previous study [1]. Each RGB component of the LSF is represented as a vector having 100 elements as input and output, and the layered layout of the 3D printer is set as the middle output. The middle output is a vector having 14 elements, each layer representing a concentration pattern of ink. The value of the element is an integer value, which indicates the number of layers where the ink will be used. Since the number of layers in the patch is 10, the sum of the vectors is also 10. The range of LSF values is 0 to 1, and the layout is normalized so that the values are ranged from 0 to 1 during training. At first, the training is done only in the decoder part, then the encoder and decoder are connected and the training is done again fixing the weight parameters of the decoder.

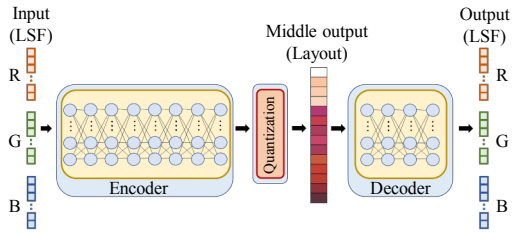

Figure. 10 *The structure of the deep neural network model*

Loss functions are provided for both the middle and the output, and RMSE is used for both. The target of this estimation is the number of layers of each ink used to print the patch, which is an integer. Since the value output from the encoder is a real number, it must be rounded into an integer, still the rounding operation is not differentiable, and this cannot be done during the training.

5.2 Training result

Using MCML, we obtained 1413 pairs of layered ink layouts for the 3D printer and LSF. We used 80% of the data as training data and 20% as test data. The training results are shown in Figure 11. In Figure 11, the horizontal axis is the number of epochs and the vertical axis is the learning curve representing the output result of the loss function. The blue line in the figure is the loss value for the training data, and the orange line is the loss value for the validation data. The training of the decoder converges quickly, and the encoder converges when the number of epochs reaches 20. It can be seen that both of them are able to estimate the validation data with sufficiently high accuracy. The loss value for the previously divided test data is 0.1460, which shows that the estimation can be made for unknown data with the same accuracy as the training data. Here, the loss value when the encoder training converges is about 0.14, which means that the difference from the ground truth in the number of layers is 1.4 layers.

5.3 Validation of the proposed method using CG data

To verify the accuracy of the neural network trained in the previous section, we created a CG skin object using Mitsuba renderer [10] and obtained the point spread function (PSF) by irradiating it with a point light source. The created skin object and the obtained PSF are shown in Figure 12. The line spread function LSF was calculated by integrating the PSF. The resulting LSF is shown in Figure 13. The LSF shown in Figure 13 was normalized so that the range is from 0 to 1 by dividing it by the maximum value. The LSF shown in Figure 13 was input to the neural network trained in the previous section. The resulting output, deformalized and returned to integer, is shown in Table 1.

Table 1. Estimation Result of Ink layer Layout for CG Skin Object

Color														
Output	7	0	1	1	0	0	0	0	0	0	0	0	0	0

In the simulation, we assumed that only one pattern of the concentration is used for each of clear ink, skin ink, and red ink to make one layout, however, it is shown in Table 1 that output is assigned to two skin colors. Theoretically, by printing the estimated layout with a 3D printer, it should be possible to create a skin patch that reproduces the input LSF. Still, in this time, it is corrected to use only one pattern of concentration from each color (clear, skin and red) to match the condition of simulation. The correction was done by putting smaller values to the largest output. Since the activation function of the output layer of the encoder of the neural network is a softmax function, the sum of the outputs is designed to be 1. However, through the soft quantization layer, the sum can be greater than or less than 1 because the output is rounded up or truncated. For this reason, the sum of the output results shown in Table 1 is less than 10. In this case, the output value is also corrected so that the total number of layers is 10 to match the simulation condition. The way of correction is to divide each output value by the sum of the output values and then reassign the number of layers according to the ratio. The final ink layer layout obtained by these corrections is shown in Table 2.

Table 2. The final ink layer layout

Color														
Output	8	0	2		0	0	0	0	0	0	0	0	0	0

Figure 14 shows the skin patch printed by a 3D printer using the layout shown in Table 2. The color of the skin patch shown in Figure 14 (a) has a close appearance to that of the CG-created skin object. The Figure 14(b) is the skin patch illuminated by the laser projector in a dark room. It can be seen that he translucency of the printed patch is close to that of the CG-created skin object.

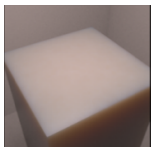

(a) Standard human skin

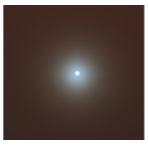

(b) PSF obtained by (a)

Figure. 12 CG-created skin object

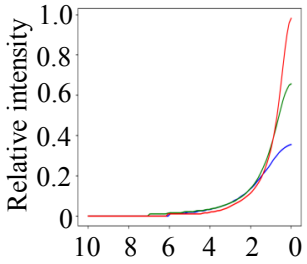

Figure. 13 LSF obtained from CG-created skin object

(a) *The printed result*

(b) *The translucency of the printed skin patch*

Figure. 14 *the skin patch printed by a 3D printer using the layout shown in table 2.*

6. Conclusions and Future Works

In this study, we focused on the optical properties of objects and proposed a method to estimate the ink layer layout to be input to a 3D printer that reproduces the desired translucency based on line spread function. We used encoder decoder type of deep neural network for the estimation. The training data fed to the neural network, which is a pair of layer structure layout and LSF, were prepared synthetically using a simulation method, MCML. The proposed method was validated using the LSF obtained from the CG data as input, and showed that the printed skin patch gives a similar appearance and translucency to the input CG skin.

It was shown that our method works and gives a reasonable result, still this research is preliminary and has considerable room for improvement. No verification has been made as to how accurate the absorption and scattering coefficients estimated from the ink samples are. To show that the printed samples using estimated parameter are close to a CG skin model in terms of color and transparency, a color index (e.g. L*a*b*) and a transparency index (TP) should be taken into account. We believe that more accurate simulation can be achieved by using a more precise measurement method to obtain accurate parameters, which is spatial Fourier Domain Imaging to obtain scattering coefficient for instance. Besides, we think it is necessary to verify that MCML is applicable to the 3D printed patch with a layer structure, and compare the simulated LSF and actual LSF given by same ink layer layout.

References

[1] Brunton Alan, Can A. Arikan and Philipp Urban. 2015. Pushing the limits of 3D color printing: Error diffusion with translucent materials. *ACM Transactions on Graphics (TOG)* 35.1 (2015): 1-13.

[2] Alan Brunton, Can A. Arikan, Tejas M. Tanksale and Philipp Urban. 2018. 3D printing spatially varying color and translucency. *ACM Transactions on Graphics (TOG)* 37.4 (2018): 1-13.

[3] Philipp Urban, Tejas M. Tanksale, Alan Brunton, Bui M. Vu and Shigeki Nakauchi. 2019. Redefining a in rgba: Towards a standard for graphical 3d printing. *ACM Transactions on Graphics (TOG)* 38.3 (2019): 1-14.

[4] Junki Yoshii, Shoji Yamamoto, Kazuki Nagasawa, Wataru Arai, Satoshi Kaneko, Keita Hirai and Norimichi Tsumura, "Estimation of Layered Ink Layout from Arbitrary Skin Color and Translucency in Inkjet 3D Printer." Color and Imaging Conference. Vol. 2019. No. 1. Society for Imaging Science and Technology, 2019.

[5] Kathrin Happel, Marius Walter, Philipp Urban, and Edgar Dörsam, "Measuring Anisotropic Light Scatter within Graphic Arts Papers for Modeling Optical Dot Gain", 18th Color and Imaging Conference, pp.347–352, 2010.

[6] Wang Lihong, Steven L. Jacques, and Liqiong Zheng., "MCML - Monte Carlo modeling of light transport in multi-layered tissues," Computer Mehtods and Programs in BIomedicine, Vol. 47, No. 2, pp. 131-146, 1995.

[7] Henrik Wann Jensen, Stephen Robert Marschner, Marc Levoy, and Pat Hanrahan, "A practical model for subsurface light transport." Proceedings of the 28th annual conference on Computer graphics and interactive techniques. ACM, 2001.

[8] Tominaga, Shoji. "Color control of printers by neural networks." Journal of Electronic Imaging 7.3 (1998): 664-672.

[9] Liang Shi, Vahid Babaei, Changil Kim, Michael Foshey, Yuanming Hu, Pitchaya Sitthi-Amorn, Szymon Rusinkiewicz and Wojciech Matusik, "Deep multispectral painting reproduction via multi-layer, custom-ink printing." ACM Transactions on Graphics (TOG) 37.6 (2019): 271.

[10] W. Jakob, Mitsuba renderer, http://www.mitsubarenderer.org, 2010.